Integrated Coherent Receivers for High-Linearity Microwave Photonic Links

Anand Ramaswamy, *Student Member, IEEE*, Leif A. Johansson, *Member, IEEE*, Jonathan Klamkin, Hsu-Feng Chou, *Member, IEEE*, Colin Sheldon, Mark J. Rodwell, *Fellow, IEEE*, Larry A. Coldren, *Fellow, IEEE, Fellow, OSA*, and John E. Bowers, *Fellow, IEEE, Fellow, OSA*

***Abstract*—In this paper, we present a coherent receiver based on an optical phase-locked loop (PLL) for linear phase demodulation. The receiver concept is demonstrated at low frequency. For high-frequency operation, monolithic and hybrid integrated versions of the receiver have been developed and experimentally verified in an analog link. The receiver has a bandwidth of 1.45 GHz. At 300 MHz, a spurious free dynamic range (SFDR) of 125 dB · Hz$^{2/3}$ is measured.**

***Index Terms*—Analog links, coherent communication, microwave photonics, phase-locked loop (PLL), phase modulation.**

I. Introduction

THE transport of analog signals over optical fiber allows for the placement of signal processing electronics away from the often exposed location of the antenna unit. The low-loss nature of fiber allows the signal to be transported over long distances with minimal signal loss. Since the transport is performed in the optical domain, the link itself is immune to electromagnetic interference. Original work on radio over fiber was considered for satellite communication applications [1]. More recent efforts have primarily focused on wireless mobile communication systems [2], where the relatively linear response of inexpensive directly modulated sources [3], [4] make moderate performance inexpensive links attractive for this application.

For higher dynamic range analog systems that require extreme linearity, radio over fiber does not currently meet the most stringent performance requirements. Direct modulation of laser diodes is a linear process, but the need for high speed modulation and very low noise at the signal frequency is difficult to meet with a single optical source. The two requirements can be decoupled if an external optical modulator is used. However, for intensity modulation the modulation depth is limited to 100% and it is difficult to fit a truly linear transfer function between zero and full transmission. In contrast, optical phase modulation can generate practically unlimited modulation depth. Many optical phase modulators also rely on the linear electrooptic effect, e.g., $LiNbO_3$ modulators. Unfortunately, there is currently a lack of techniques for linear phase demodulation. A standard optical mixing based phase detector has a sinusoidal response which then limits the link performance [5].

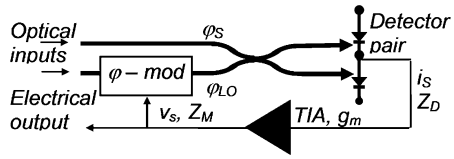

Fig. 1. Schematic outline of receiver architecture.

In this paper, we describe a technique for linear optical phase demodulation using an optical phase locked loop [6]. The paper is organized as follows. In Section II the operating principle of the phase detector is outlined and a basic analytical model is developed to reveal the limits of performance of the phase detector. The next section summarizes a proof-of-principle system demonstration built using discrete components at low frequency. Section IV introduces the development of a high-speed integrated optical phase receiver. The following section describes the performance of the subcomponents of the receiver, before the link results using the integrated receiver are shown in Sections VII and VIII.

II. Theory

The base function of the proposed receiver is shown in the diagram of Fig. 1. The receiver is built around a standard optical mixing based phase detector with a differential output signal current given by

$$i_S = 2R\sqrt{P_S P_{\mathrm{LO}}}\sin(\varphi_S - \varphi_{\mathrm{LO}}) \tag{1}$$

Where P_S and P_{LO} are signal and LO optical power, φ_S and φ_{LO} are optical phase and R is the responsitivity of the detector. This signal is then amplified to form a driving voltage to a tracking optical phase modulator

$$v_S = Z_D \cdot g_m \cdot Z_M \cdot i_S \tag{2}$$

where Z_D, Z_M are detector and modulator impedances and g_m is the amplifier transimpedance. Finally, the feedback phase is given by

$$\varphi_{\mathrm{LO}}(t) = \frac{\pi}{V_{\pi,R}} \cdot v_s \tag{3}$$

Manuscript received June 29, 2007; revised September 21, 2007. This work was supported by the DARPA PHOR-FRONT program under the United States Air Force Contract FA8750-05-C-0265.

A. Ramaswamy, L. A. Johansson, C. Sheldon, M. J. Rodwell, L. A. Coldren, and J. E. Bowers are with the Department of Electrical and Computer Engineering, University of California, Santa Barbara, CA 93106 USA (e-mail: anand@ece.ucsb.edu).

J. Klamkin is with the Materials Department, University of California, Santa Barbara, CA 93106 USA (e-mail: klamkin@engineering.ucsb.edu).

H.-F. Chou was with the Department of Electrical and Computer Engineering, University of California, CA 93106 USA. He is now with Luminent OIC Inc., Chatsworth, CA 91311 USA (e-mail: Hsu-Feng.Chou@ieee.org).

Color versions of one or more figures are available at http://ieeexplore.ieee.org.

Digital Object Identifier 10.1109/JLT.2007.911899

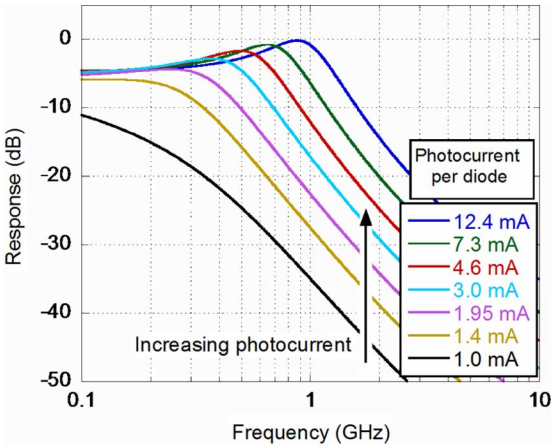

Fig. 2. Simulated close loop response of receiver.

where $V_{\pi,R}$ is the half wave voltage of the reference modulator. For a linear phase modulator and for close phase tracking, i.e., when the feedback gain is large and $\varphi_S \approx \varphi_{\rm LO}$, the reference modulator drive signal, v_S will be linearly related to the input phase and forms the linear output signal from the receiver.

The receiver forms a classic feedback system where the Laplace transform can be applied. The sine component in (3) can be linearized and the LO phase is given by

$$\begin{aligned}\varphi_{\rm LO} &= \frac{\pi}{V_{\pi,R}} Z_D(s)\cdot g_m(s)\\ &\quad\times \cdot Z_M(s)\cdot 2R\sqrt{P_S P_{\rm LO}}\cdot {\rm K}\\ &\quad\times {\rm K}\cdot e^{-s\tau}(\varphi_S-\varphi_{\rm LO})\\ &= T(s)\cdot(\varphi_S-\varphi_{\rm LO}) \end{aligned} \tag{4}$$

where $s = 2\pi$ if is the Laplace variable, T is the open-loop gain and τ is the delay of the feedback path, now appearing in an exponential term. The delay will add a phase lag at higher frequencies and to prevent oscillation in the feedback loop, the feedback gain must be below unity at the frequency where the phase crosses $-180°$. This forms the basic bandwidth limitation in the loop such that to generate a fast feedback loop at microwave frequencies, picosecond feedback delay is required.

The closed-loop response given by $H = T/(1+T)$ can be calculated from the open-loop transfer function. The overall optical link response using the closed-loop receiver can now be calculated. Fig. 2 shows an example of such a calculation where an effort has been made to use measured data from Section VI to derive the component performance parameters that contribute to the open-loop transfer function.

This feedback loop differs from a typical optical phase-lock loop in that an optical modulator is used instead of a current controlled oscillator (CCO) in the form of a frequency tuned laser [7]. Here, the phase tracking range is limited by the available phase swing across the reference modulator. This limitation can be overcome by implementing an additional, slow loop to extend the tracking range, and/or having an LO input that is coherent in phase with the unmodulated signal input. The lack of a CCO removes an integration in the loop that needs to be compensated for. This can be implemented by tailoring the frequency dependence of the transimpedance amplifier to provide the right feedback response. A better solution is to rely on the detector and modulator impedances. By taking advantage of the detector and modulator capacitances, two integrations are automatically formed and the feedback amplifier now only needs to incorporate a lag-compensation network for stability in order to form a second-order phase-locked loop. This leads to greatly improved efficiency, in that no matching resistors need to be used to generate a flat detector and modulator frequency response. In fact, for sufficiently high photocurrent values, it becomes possible to not use any transimpedance amplification in the feedback path but to instead rely on a direct interconnect between modulator and detector to realize a first-order loop with a single pole formed by the detector in parallel with the modulator impedance.

III. Proof of Concept Demonstration

In order to explore the feasibility of the proposed receiver and demonstrate that closure of the feedback path results in a significant enhancement of linearity without any penalty in SNR, a proof of principle experimental setup was built [8]–[10]. The operating frequency is limited to the 100 KHz range due to the relatively large loop delays introduced by the fiber patch cords of the discrete components used in the receiver.

The experimental arrangement for this approach is outlined in Fig. 3. The output from a continuous-wave (CW) optical source is split into a signal path and a reference path using a polarizing beam splitter (PBS) and polarization maintaining fiber. A two-tone RF probe signal (140 KHz and 160 KHz) is applied separately to the $LiNbO_3$ phase modulators at the transmitter. In the receiver, the signals from the two paths are mixed and photodetected. The optical mixer is composed of a single-polarization optical coupler and a balanced photodetector. PM4 is the local phase modulator that provides feedback. The load of the balanced photodetector is 100 pf in parallel with the parallel combination of 2.96 kΩ and 20 kΩ. PM3 is driven by a slow feedback circuit that tracks large but slow variations in phase caused by the environment around the setup and uses it to maintain the bias of the demodulator at quadrature. A first-order RC filter is added to the output stage to suppress any noise generated by the stabilization electronics from entering the signal loop. A more detailed description of the experiment can be found in [11].

When the photocurrent from the balanced photodetector is large enough, say a few mA, several volts of voltage swing can be obtained with a high impedance load. This is sufficient to drive the $LiNbO_3$ reference modulators on the LO branch and consequently eliminates the need for electrical loop amplifiers, forming an "all-optical" loop as described in the previous section. The frequency dependence of the load now determines the loop filter function. It is worth noting that the balanced modulator configuration described in Section V and implemented in the integrated version of the receiver is not realized in the discrete setup.

Fig. 4 plots the power of the detected fundamental and intermodulation terms as a function of the input link power. The stabilization loop remains closed for both open and closed loop operation. A SFDR of 104.5 dB $\cdot$ Hz$^{2/3}$ is obtained for open loop operation.

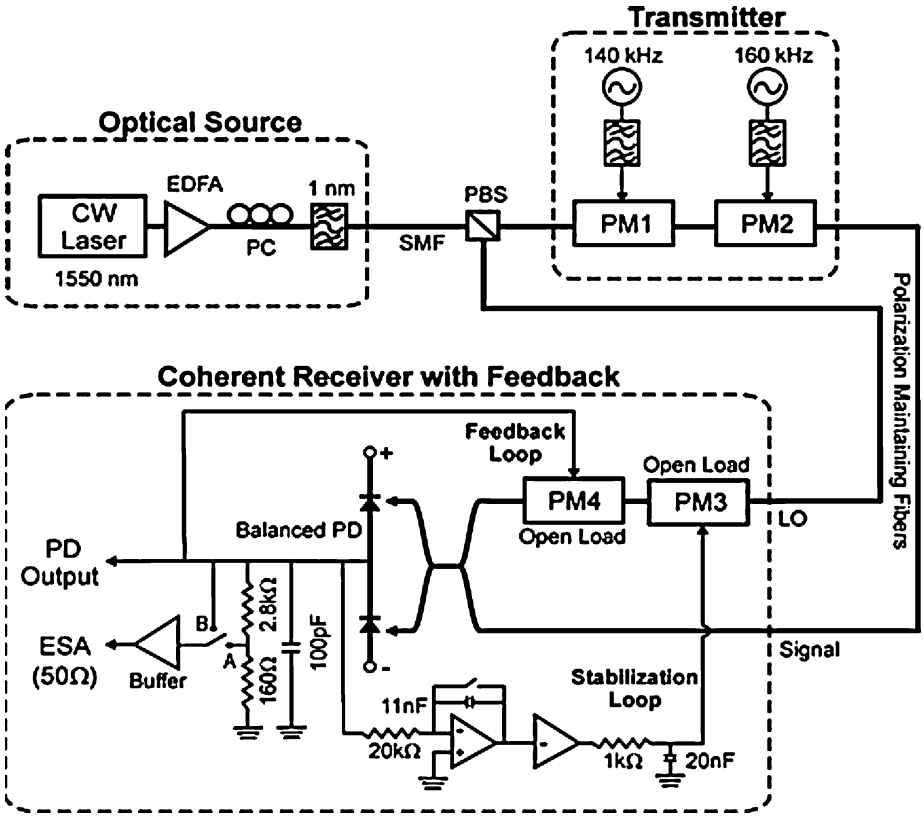

Fig. 3. Experimental setup of the all photonic version of the proposed coherent receiver. ESA: Electrical Spectrum Analyzer; PD: photodetector.

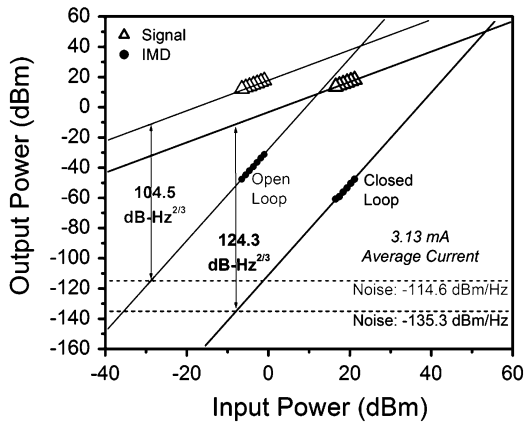

Fig. 4. SFDR measurement at 3.13 mA of average photocurrent per detector. Gray: open loop; Black: closed loop. IMD: third-order intermodulation distortion.

When the loop is closed a number of effects are observed. First, there is a significant decrease in the detected power on account of the reduced net phase swing across the demodulator. However, as predicted, this is not accompanied by any degradation in SNR as the noise floor too is suppressed by the same factor. The second effect is a drastic reduction of the intermodulation terms that appear at 120 and 180 KHz. This translates into an improvement in SFDR by about 20 to 124.3 dB $\cdot$ Hz$^{2/3}$. The calculation of shot noise power when the loop is closed is complicated by the feedback effect. Essentially, the shot noise current manifests itself as phase shot noise at the reference modulator. This in turn appears as voltage shot noise at the ouput of the balanced PD. With the buffer switch in position B (Fig. 3) the shot noise power is measured on a Electrical Spectrum Analyzer (ESA) that has a 50-Ω termination. It is observed that the measured noise levels are approximately 10 dB higher than the theoretical shot noise limit. As a consequence of operating at low frequencies, the difference can be attributed to the $1/f$ noise contributions from the optical source. The proof of concept demonstrations of the optoelectronic and all photonic feedback receivers is the first step towards realizing a receiver that has an operating bandwidth in the gigahertz range. Such a receiver requires low feedback delay (< 10 ps) and consequently, hybrid or monolithic integration of electronics and photonics is necessary [12].

IV. Integrated Receiver Development

To reach microwave frequencies the latency in the loop needs to be small. In the proof-of-principle demonstration above using fiber optics, component length of several meters produced a loop operating frequency of $\sim$ 100 kHz. Using two orders of magnitude more compact $LiNbO_3$ waveguiding would produce a low operating frequency on the order of 10 MHz. To reach microwave frequencies of around 1 GHz, a waveguiding platform four orders of magnitude more compact than fiber optics must be used with component lengths in the 100s of microns region. This is being satisfied using an InP photonic integration platform.

Fig. 5 shows an SEM and block diagram of the low latency feedback receiver comprising of a photonic integrated circuit

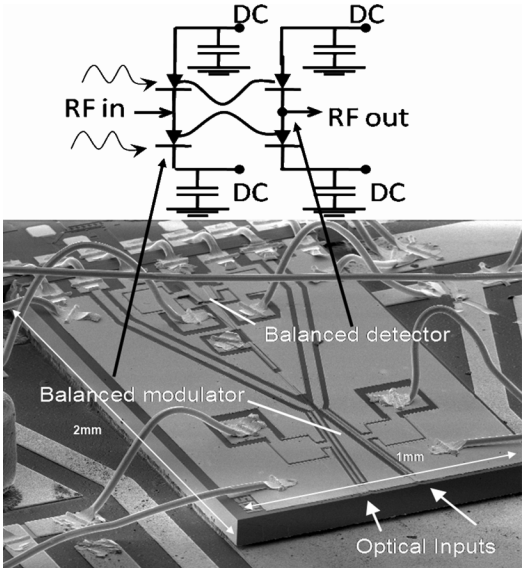

Fig. 5. SEM and block diagram of Integrated Optoelectronic Receiver: Wire bonds in upper part connect to Integrated Electronic IC (not shown).

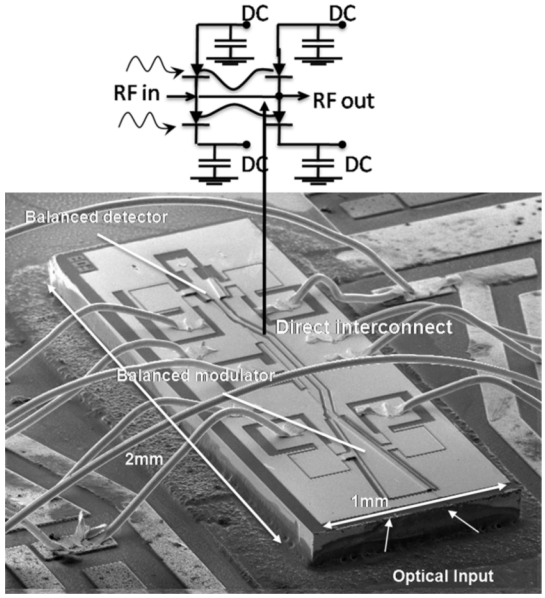

Fig. 6. SEM and block diagram of Integrated All-Photonic receiver.

and an electronic integrated circuit. The InP based photonic IC consists of a balanced UTC photodetector pair [13], a 2×2 waveguide multimode interference (MMI) coupler and tracking phase modulators in a balanced configuration. In quadrature, this type of balanced receiver discriminates against common-mode and second-order nonlinearities. The tracking optical phase modulators are *driven* differentially so as to add opposite-sign phase shifts to the incoming signal and LO resulting in a cancellation of even-order nonlinearities and common-mode noise. Additionally, driving the modulators in a differential fashion doubles the drive voltage presented to the modulator thereby doubling the available phase swing. The capacitances of the photodiodes and modulators are exploited as circuit elements rather than being parasitics that need to be eliminated. These now perform the desired loop integrations and can therefore be much larger. The electronic chip that interfaces with the PIC is primarily a transconductance amplifier that converts the voltage generated by photodiode integration into a modulator drive current. The modulator integrates this current to produce the required phase shift. The electronic IC also has a pair of buffer amplifier capable of driving 50 ohms. The electronic chip finally contains a lag compensation circuit to improve the phase margin and provide stability to the system.

Because the detector and modulator capacitances are implemented as lumped elements and best operate as ideal current mode integrators, a high-gain version of the receiver that requires no electronics in the feedback path is feasible. The detector photocurrent drives the sum of the photodiode and modulator capacitance, generating a voltage that is proportional to the photocurrent. As the received photocurrent increases, lower gain is required from the electronic amplifiers in the phased locked loop. Subsequently, for sufficiently high photocurrents the modulator impedance can be tailored to provide adequate filtering and stable phase feedback so that it can be driven directly by the detector photocurrent, similar to the proof-of concept demonstration in Section III. An SEM and block diagram of this all photonic receiver is shown in Fig. 6. Note that an electronic chip is still required to provide a buffered output.

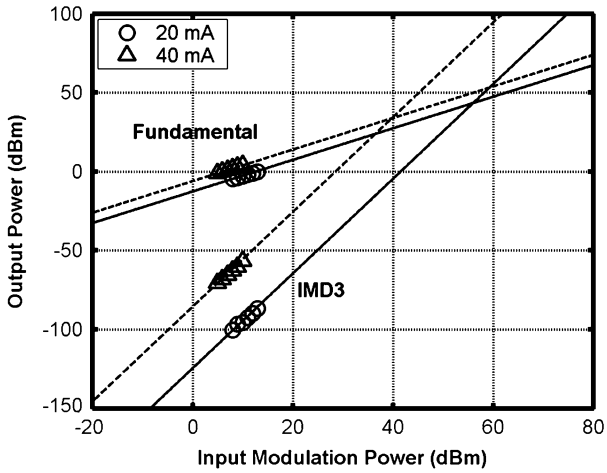

Fig. 7. IMD3 measurements for a 10 μm $\times$ 150 μm UTC-PD. At 20 mA the bias voltage is -8 V and at 40 mA the bias voltage is -5.8 V.

The practical challenge in taking full advantage of the linearity of a phase modulated link stems from stringent performance requirements on the detectors and modulators.

V. Modulator and Detector Performance

In the low frequency, all photonic demonstrator, the SFDR obtained was limited by the maximum amount of photocurrent (3.13 mA per detector) and linear voltage swing that could be detected without degradation in linearity. It is predicted that if this number can be increased to 100 mA then 138–148 dB $\cdot$ $Hz^{2/3}$ of SFDR can be realized. However, this means that highly linear photodiodes must be used with output IP3 performance on the order of 50 dBm at this photocurrent. Fig. 7 shows the OIP3 of the UTC photodiode used in the receiver. A 10 μm $\times$ 150 μm UTC-PD has a saturation current greater than 40 mA

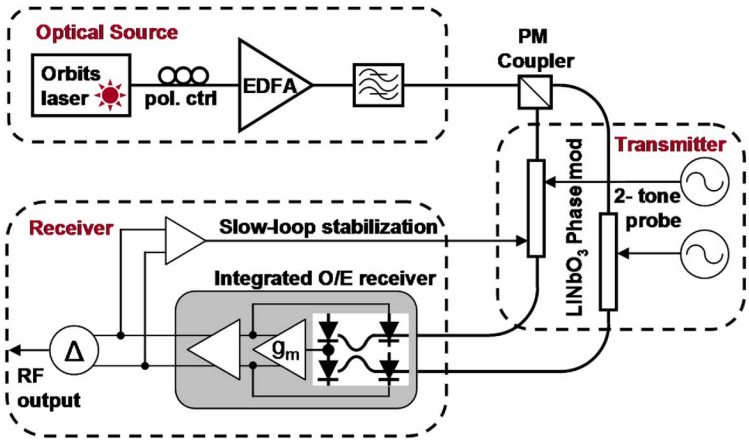

Fig. 8. Schematic of Experimental setup for Link Experiment.

and OIP3 values of 43 and 34 dBm at photocurrent levels of 20 and 40 mA, respectively [14].

A second critical performance requirement is the linearity of the phase modulators. While closed-loop operation suppresses nonlinearities from the optical interferometer as well as the amplifier, any nonlinear response of the phase modulator will remain. Since the feedback loop will force the reference phase to closely track the signal phase, a nonlinear phase modulator will consequently be modulated by a nonlinear drive signal. Using linear $LiNbO_3$ phase modulators, this is not a limiting problem. However, Stark effect InP phase modulators predominantly rely on the more efficient quadratic electrooptic effect. The high efficiency leads to very short modulator structures and low latency, but the linearity of a single modulator will limit the available receiver performance.

An improved modulator configuration is obtained by placing two phase modulators, one in the signal arm and one in the LO arm, in a push-pull configuration. These are now driven in antiphase. The compound response is now given by

$$\begin{aligned}\varphi_m &= \varphi_1(v_m) - \varphi_2(-v_m) \\ &= \sum_n a_n v_m^n - \sum_n a_n(-v_m)^n \\ &= \sum_{n'} 2a_{2n'+1} v_m^{2n'+1} \end{aligned} \tag{5}$$

Where φ_m and v_m are the modulation phase and drive voltage, respectively, and a_n is the Taylor expansion coefficient around the modulator bias point. It is seen that the quadratic term along with any higher even-order terms are cancelled using this configuration. A second beneficial effect is that the amplitude modulation from the phase modulators is to a first-order approximation cancelled [15].

VI. Analog Link Experiment

The performance of both receivers was evaluated by placing them in an experimental test bed that simulates an analog link [14]. The setup, shown in Fig. 8, is similar to the configuration described earlier for the low-frequency demonstration. However, a few modifications have to be made in order for the system to handle the high optical powers (20–28 dBm) used in the link experiment. For instance, a 100-GHz DWDM drop filter rated to 5 W is used instead of an optical bandpass filter. Additionally, a 50/50 polarization maintaining (PM) coupler replaces the polarizing beam splitter (PBS).

At the transmitter, a two tone drive signal is applied separately to $LiNbO_3$ Phase modulators that have V_π's of 4.4 and 5.5 V respectively. This ensures the spectral purity of the drive signals as the closely spaced RF tones ($\Delta f = 2$ MHz) are combined in the optical domain.

At the output of the receivers the differential signal is tapped into a slow feedback loop which generates a low-frequency drive signal to one of the phase modulators. This stabilizes the system against environmental drifts and maintains the bias of the phase demodulator at quadrature. Ideally, the stabilization circuit should be located in the receiver module. However, for experimental convenience it is driving the phase modulator at the transmitter.

The box labeled 'Integrated O/E receiver' shows a schematic of the photonic integrated circuit coupled with the transimpedance amplifier and buffer of the electronic integrated circuit used in the optoelectronic (O/E) version of the receiver. The differential output from the amplifier drives the reference modulators on the PIC. The RF outputs sensed from the buffer constitute the receiver's output. They are 180° out of phase and are combined differentially.

VII. Frequency Response

A. Optoelectronic Receiver

The effect of the feedback architecture is to suppress the net phase swing across the detector by a factor of $(1/1+T)$ where T is the Loop Transmission Gain. Fig. 9 plots the closed loop frequency response of the receiver at different levels of detected photocurrent.

From theory we know that when the loop is locked and the reference modulator is closely tracking the incoming phase, the link gain is determined by the ratio of the drive signals to the source and reference modulator. This can be observed at low frequencies for a wide range of photocurrents. As the frequency

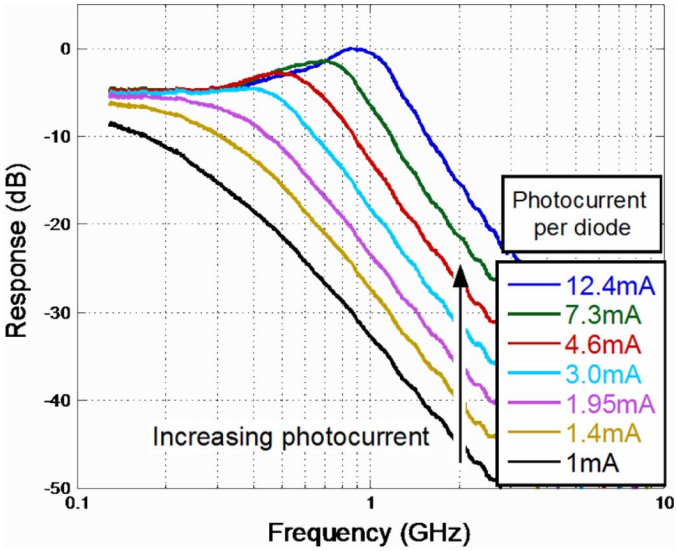

Fig. 9. Link gain of optoelectronic receiver at varying photocurrent levels.

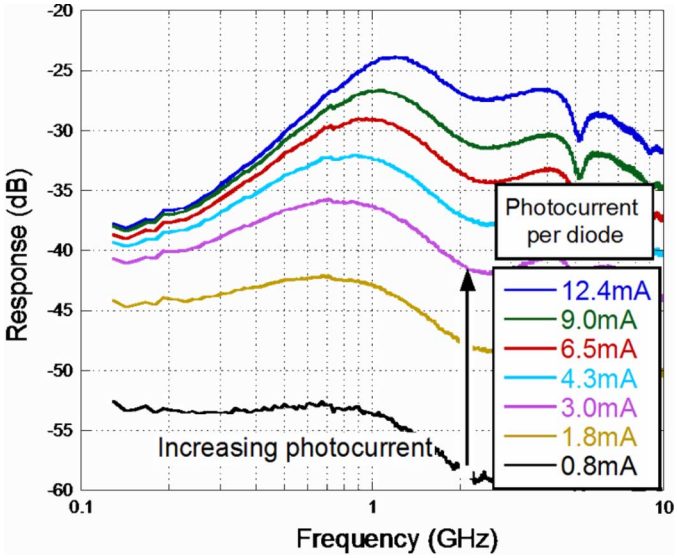

Fig. 10. Link gain of all-photonic receiver at varying photocurrent levels.

increases, the feedback gain decreases and only at high photocurrent levels is the gain sufficient for phase tracking. Beyond a point, the loop transmission gain is too low for any tracking and consequently, the optical link gain becomes proportional to the photocurrent and loop filter transfer function. The loop bandwidth, here defined as the 3 dB frequency of the closed-loop link response, reaches 1.45 GHz at 12 mA of photocurrent. The delay limited bandwidth, within which the loop remains stable is approximately 4 GHz. Additionally, we note a peaking in the link gain for high photocurrent values at frequencies close to a GHz. This can be explained by the denominator in the closed-loop gain, $1 + T$. A second-order feedback loop contains two integrations with a -180° feedback phase. To provide stability at unity gain, the transimpedance amplifier contains a lag-compensating network to push the phase well above -180° at unity gain. This has been designed for delay-limited feedback gain and does therefore not provide optimum lag-compensation at around 1 GHz.

B. All Photonic Receiver

The operation of the all photonic receiver differs from the optoelectronic receiver in that the efficiency of the modulators is sufficiently high for them to be driven by the absorbed RF photocurrent alone. The modulators are operated under forward bias and have an I_π of approximately 10 mA below 100 MHz. Fig. 10 shows the measured link response using this receiver. In the optoelectronic receiver when the incoming phase is being tracked closely by the reference modulator, the response is flat and determined by the drive voltage ratio to the source and reference modulator. In the all photonic receiver the response when the loop is closed varies with frequency. This is observed in the plot in Fig. 10 and can be attributed to the frequency dependence of the I_π of the modulator. The link gain is still related to the ratio of V_π between source and reference modulator. For a forward biased modulator, the diode impedance is typically very low (10–15 Ω) and requires a very small drive voltage, overall resulting in a much lower link gain than when a reverse biased reference modulator is used.

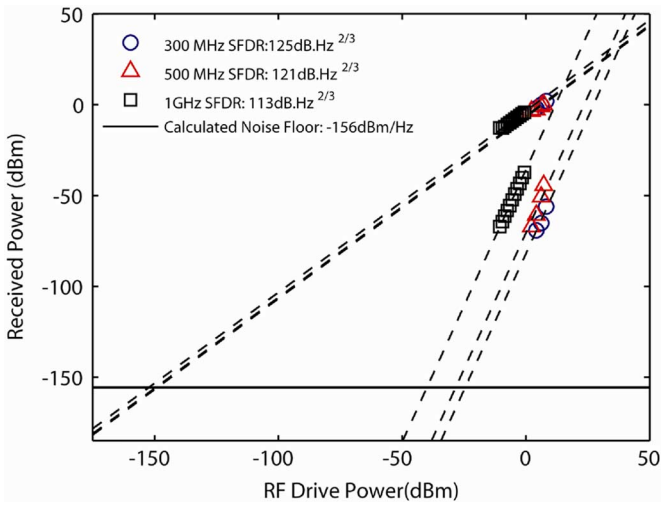

Fig. 11. SFDR of optoelectronic receiver at 300 MHz, 500 MHz and 1 GHz. Photocurrent set at 12 mA per detector.

VIII. SFDR Measurement

Using the Link Setup of Fig. 8, a two tone SFDR measurement is made on the optoelectronic receiver at three different frequencies with the same photocurrent (12 mA) in each detector. The results of this measurement are shown in Fig. 11. In Section VI we observed that the loop gain is higher at lower frequencies. Hence, the reference modulator can better track the incoming signal phase and consequently the SFDR is much higher at 300 MHz (125 dB $\cdot$Hz$^{2/3}$) than at 500 MHz or 1 GHz. As the loop gain decreases there is a diminishing reduction in the net received phase and at 1 GHz the reduction is negligible. Thus, the SFDR measured (113 dB $\cdot$Hz$^{2/3}$) corresponds closely to the open loop SFDR at that frequency. The noise floor shown is the

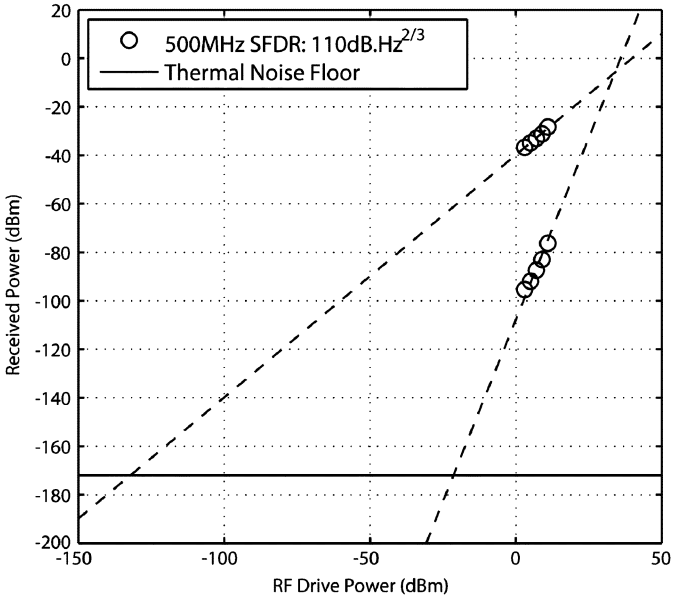

Fig. 12. SFDR of all photonic receiver at 500 MHz and 15 mA of photocurrent per detector.

calculated shot noise level. In practice, the noise floor is determined by the ASE of the high-power EDFA (30 dB gain, 5.5 dB NF) that was used to provide the required optical power. It is estimated that if a low-noise, high power laser is used, shot-noise limited operation should be available at this photocurrent level.

Fig. 12 shows a similar SFDR measurement made at 500 MHz on the all photonic receiver. The SFDR is considerably lower (110 $\mathrm{dB}\cdot\mathrm{Hz}^{2/3}$) when compared to the SFDR at 500 MHz (121 $\mathrm{dB}\cdot\mathrm{Hz}^{2/3}$) for the optoelectronic receiver. Shot-noise limited performance is also not available for this receiver configuration. Since the on chip reference modulators are forward biased their drive voltage is low and consequently, the buffer amplifer noise is higher than the drive signal to the modulator needed to suppress the shot noise of the receiver. In the receiver, thermal noise dominates over the shot noise at the received photocurrent (15 mA). An effort is being made to realize lower loss and hence, higher receiver photocurrent and loop gain for both the optoelectronic and all-photonic receiver architectures.

IX. Conclusion

In this paper, we have described and experimentally demonstrated a coherent integrated receiver that is based on a broadband optical phased locked loop. The delayed limited bandwidth of the loop is 4 GHz. In order to port the link to a much higher carrier frequency, we are exploring the idea of optical sampling [17]–[21]. Additionally, the PLL bandwidth of 1.45 GHz demonstrated here would be sufficiently large to track the phase noise of standard semiconductor lasers with low phase error.

Acknowledgment

The authors would like to thank helpful discussions with Larry Lembo, Darko Zibar, Steve Pappert, and Jim Hunter. Northrop Grumman Space Technologies are acknowledged for providing the electronic IC.

References

[1] J. E. Bowers, A. C. Chipaloski, S. Boodaghians, and J. W. Carlin, "Long distance fiber-optic transmission of C-band microwave signals to and from a satellite antenna," *J. Lightw. Technol.*, vol. LT-5, pp. 1733–1741, 1987.

[2] D. Wake, M. Webster, G. Wimpenny, K. Beacham, and L. Crawford, "Radio over fiber for mobile communications," in *Proc. Microw. Photon. (MWP'04)*, Oct. 2004, pp. 157–160.

[3] A. Larsson, C. Carlsson, J. Gustavsson, A. Haglund, and P. Modh, "Broadband direct modulation of VCSELs and applications in fiber optic RF links," presented at the Proc. IEEE Int. Topical Meet. Microw. Photon., Oct. 2004, paper WA-1, unpublished.

[4] P. Hartmann *et al.*, "Demonstration of highly linear uncooled DFB lasers for next generation RF over fibre applications," in *Proc. 28th European Conf. Opt. Commun. (ECOC)*, 2002, vol. 2, pp. 1–2.

[5] F. Bucholtz, V. J. Urick, M. S. Rogge, and K. J. Williams, "Performance of analog photonic links employing phase modulation," presented at the Proc. OSA Topical Meet. Coherent Opt. Technol. Applicat. (COTA), 2006, Paper CFA6, unpublished.

[6] Y. Li *et al.*, "Receiver for a coherent fiber-optic link with high dynamic range and low noise figure," in *Proc. Int. Top. Meet. Microw. Photon. (MWP'05)*, Seoul, Korea, 2005.

[7] M. Ohtsu, *Highly Coherent Semiconductor Lasers*. Norwood, MA: Artech House, 1992.

[8] H. F. Chou, A. Ramaswamy, D. Zibar, L. A. Johansson, J. E. Bowers, M. Rodwell, and L. A. Coldren, "SFDR improvement of a coherent receiver using feedback," presented at the Proc. OSA Top. Meet. Coherent Opt. Techn. Applicat. (COTA), Whistler, BC, 2006, Paper CFA3, unpublished.

[9] H. F. Chou, L. A. Johansson, D. Zibar, A. Ramaswamy, M. Rodwell, and J. E. Bowers, "All-optical coherent receiver with feedback and sampling," in *Proc. Int. Top. Meet. Microw. Photon. (MWP'06)*, Grenoble, France, 2006.

[10] G. E. Betts, W. Krzewick, S. Wu, and P. K. L. Yu, "Experimental demonstration of linear phase detection," *IEEE Photon. Technol. Lett.*, vol. 19, no. 1 3, pp. 993–995, Jul. 2007.

[11] H. F. Chou, A. Ramaswamy, D. Zibar, L. A. Johansson, J. E. Bowers, M. Rodwell, and L. A. Coldren, "High-linearity coherent receiver with feedback," *IEEE Photon. Technol. Lett.*, vol. 19, no. 12, pp. 940–942, Jun. 2007.

[12] M. N. Sysak, J. W. Raring, J. S. Barton, M. Dummer, A. Tauke-Pedretti, H. N. Poulsen, D. J. Blumenthal, and L. A. Coldren, "Single-chip, widely-tunable 10 Gbit/s photocurrent-driven wavelength converter incorporating a monolithically integrated laser transmitter and optical receiver," *Electron. Lett.*, vol. 42, no. 11, pp. 657–658, May 2007.

[13] J. Klamkin *et al.*, "Monolithically integrated balanced uni-traveling-carrier photodiode with tunable MMI coupler for microwave photonic circuits," in *Proc. Conf. Optoelectron. Microelectron. Mater. Dev. (COMMAD)*, Perth, Australia, Dec. 2007.

[14] J. Klamkin *et al.*, "High output saturation and high-linearity uni-traveling-carrier waveguide photodiodes," *IEEE Photon. Technol. Lett.*, vol. 19, no. 3, pp. 149–151, Feb. 2007.

[15] L. A. Johansson, H. F. Chou, A. Ramaswamy, J. Klamkin, L. A. Coldren, M. J. Rodwell, and J. E. Bowers, "Coherent optical receiver for linear optical phase demodulation," in *Proc. IEEE MTT-S Int. Microw. Symp.*, Honolulu, Hawaii, Jun. 2007.

[16] A. Ramaswamy, L. A. Johansson, J. Klamkin, C. Sheldon, H.-F. Chou, M. J. Rodwell, L. A. Coldren, and J. E. Bowers, "Coherent receiver based on a broadband optical phase-lock loop," presented at the Optical Fiber Communications Conference (OFC) Postdeadline Technical Digest. Opt Soc., 2007, Paper PDP3, unpublished.

[17] P. W. Juodawlkis, J. C. Twichell, G. E. Betts, J. J. Hargreaves, R. D. Younger, J. L. Wasserman, F. J. O'Donnell, K. G. Ray, and R. C. Williamson, "Optically sampled analog-to-digital converters," *IEEE Trans. Microw. Theory Tech.*, vol. 49, pp. 1840–1852, 2001.

[18] P. W. Juodawlkis, J. J. Hargreaves, R. D. Younger, G. W. Titi, and J. C. Twichell, "Optical down sampling of wideband microwave signals," *J. Lightw. Technol.*, vol. 21, no. 12, pp. 3116–3124, Dec. 2003.

[19] D. Zibar, L. A. Johansson, H. F. Chou, A. Ramaswamy, M. Rodwell, and J. E. Bowers, "Novel optical phase demodulator based on a sampling phase-locked loop," *IEEE Photon. Technol. Lett.*, vol. 19, no. 9, pp. 686–688, May 2007.

[20] D. Zibar, L. A. Johansson, H. F. Chou, A. Ramaswamy, M. Rodwell, and J. E. Bowers, "Investigation of a novel optical phase demodulator based on a sampling phase-locked loop," in *Proc. Int. Top. Meet. Microw. Photon. (MWP'06)*, Grenoble, France, 2006.

[21] L. A. Johansson, D. Zibar, A. Ramaswamy, L. Coldren, M. Rodwell, and J. E. Bowers, "Analysis of sampled optical phase-lock loops," in *Proc. MWP'07*, submitted for publication.

Anand Ramaswamy (S'06) received the B.S. degree in electrical engineering with a minor in physics and the M.S. degree in electrical engineering from the University of Southern California, Los Angeles, and the University of California, Santa Barbara, in 2005 and 2007, respectively. He is currently working towards the Ph.D. degree under Professor John E. Bowers at the University of California, Santa Barbara.

His research interests are in coherent communication systems and nonlinear mechanisms in high-power photodetectors.

Leif A. Johansson received the Ph.D. degree in engineering from University College London, U.K., in 2002.

He accepted a Postdoctoral position at the University of California at Santa Barbara in 2002. His current research interests include design and characterization of integrated photonic devices for analog and digital applications. He is a member of the IEEE.

Jonathan Klamkin received the B.S. degree in electrical and computer engineering from Cornell University, Ithaca, NY, in 2002, the M.S. degree in electrical and computer engineering from the University of California, Santa Barbara (UCSB), in 2004, and is currently working toward the Ph.D. degree in materials at UCSB.

His research interests include the design, epitaxial growth, fabrication, and characterization of widely tunable semiconductor lasers, photodetectors, optical intensity and phase modulators, compact couplers, and semiconductor optical amplifiers for InP-based photonic integrated circuits. Currently, his efforts are focused on novel coherent integrated receivers for highly linear fiber microwave photonic links.

Hsu-Feng Chou (S'01–M'06) received the B.S. degree in physics and the M.S. degree in electrooptical engineering from the National Taiwan University (NTU), Taipei, Taiwan, R.O.C., in 1996 and 1998, respectively, and the Ph.D. degree in electrical and computer engineering from the University of California, Santa Barbara (UCSB) in 2005, where his research focused on high-speed optical communication systems.

From 1998 to 2000, he was an Engineering Officer in the R.O.C. Navy. From 2005 to 2006, he was a Postdoctoral Fellow at UCSB, with research interests in coherent RF photonic links and dynamically reconfigurable optical packet switching. He is currently with LuminentOIC Inc.,Chatsworth, CA. He has authored or coauthored over 50 papers published in various journals and conference proceedings.

Colin Sheldon received the Sc.B. degree in electrical engineering from Brown University, Providence, RI, in 2004 and the M.S. degree in electrical engineering from the University of California, Santa Barbara, in 2006. He is currently pursuing the Ph.D. degree in electrical engineering at the University of California, Santa Barbara, under the supervision of Prof. Mark Rodwell.

His research interests include high-speed circuit design, coherent optical communications, and wireless communication links.

Mark J. Rodwell (F'03) received the B.S. degree from the University of Tennessee, Knoxville, in 1980, the M.S.and Ph.D. degrees from Stanford University, Stanford, CA, in 1982 and 1988, respectively.

He is Professor and Director of the UCSB Nanofabrication Laboratory and the NSF Nanofabrication Infrastructure Network (NNIN) at the University of California, Santa Barbara. He was with AT&T Bell Laboratories, Whippany, NJ, from 1982 to 1984. His current research focuses on high-bandwidth InP bipolar transistors, compound semiconductor field-effect transistors for VLSI applications, and millimeter-wave integrated circuit design in both silicon VLSI and III–V processes.

Dr. Rodwell was the recipient of a 1989 National Science Foundation Presidential Young Investigator award and for his work on GaAs Schottky-diode ICs for subpicosecond/millimeter-wave instrumentation, he was awarded the 1997 IEEE Microwave Prize.

Larry A. Coldren (S'67–M'72–SM'77–F'82) received the Ph.D. degree in electrical engineering from Stanford University, Stanford, CA, in 1972.

He is the Fred Kavli Professor of Optoelectronics and Sensors at the University of California, Santa Barbara, CA. After 13 years in the research area at Bell Laboratories, he joined UC-Santa Barbara in 1984, where he now holds appointments in Materials and Electrical and Computer Engineering, and is Director of the Optoelectronics Technology Center. In 1990, he cofounded Optical Concepts, later acquired as Gore Photonics, to develop novel VCSEL technology; and in 1998 he cofounded Agility Communications, recently acquired by JDSU, to develop widely tunable integrated transmitters. He has authored or coauthored over 800 papers, five book chapters, one textbook, and has been issued 61 patents. He has presented dozens of invited and plenary talks at major conferences.

Prof. Coldren is a Fellow of the Institution of Electrical Engineers (IEE) and Fellow of the Optical Society of America (OSA). He is the recipient of the 2004 John Tyndall Award and a member of the National Academy of Engineering.

John E. Bowers (F'04) received the M.S. and Ph.D. degrees from Stanford University, Stanford, CA.

He is a Professor in the Department of Electrical Engineering, and in the Technology Management Program at the University of California, Santa Barbara. He is also CTO and cofounder of Calient Networks. His research interests are primarily concerned with silicon photonics, optoelectronic devices, optical switching, and transparent optical networks. He is cofounder of the Center for Entrepreneurship and Engineering Management, and founder of Terabit Technology. Previously, he had worked for AT&T Bell Laboratories and Honeywell before joining UCSB. He has published eight book chapters, 400 journal papers, 600 conference papers, and has received 49 patents.

Dr. Bowers is a Fellow of the Optical Society of America (OSA) and the American Physical Society, and a recipient of the IEEE LEOS William Streifer Award and the South Coast Business and Technology Entrepreneur of the Year Award. He was an elected member of the IEEE LEOS Board of Governors, a LEOS Distinguished Lecturer, and Vice President for Conferences for LEOS. He is a member of the National Academy of Engineering. He received the ACE Award for Most Promising Technology for the hybrid silicon laser in 2007.